Robust Spectral π Pairing in the Random-Field Floquet Quantum Ising Model

Harald Schmid[1], Alexander-Georg Penner,[1] Kang Yang[1], Leonid Glazman,[2] and Felix von Oppen[1]

[1]*Dahlem Center for Complex Quantum Systems, Freie Universität Berlin, 14195 Berlin, Germany*
[2]*Department of Physics, Yale University, New Haven, Connecticut 06520, USA*

Motivated by an experiment on a superconducting quantum processor [X. Mi *et al.*, Science **378**, 785 (2022).], we study level pairings in the many-body spectrum of the random-field Floquet quantum Ising model. The pairings derive from Majorana zero and π modes when writing the spin model in Jordan-Wigner fermions. Both splittings have log-normal distributions with random transverse fields. In contrast, random longitudinal fields affect the zero and π splittings in drastically different ways. While zero pairings are rapidly lifted, the π pairings are remarkably robust, or even strengthened, up to vastly larger disorder strengths. We explain our results within a self-consistent Floquet perturbation theory and study implications for boundary spin correlations. The robustness of π pairings against longitudinal disorder may be useful for quantum information processing.

Introduction.—The quantum Ising model [1] appears at the crossroads of many current developments in condensed matter physics and quantum information. It is paradigmatic for symmetry breaking quantum phase transitions in its spin incarnation [2,3], for topological quantum phase transitions in its fermionized version [4], and for lattice gauge theory as well as topological quantum error correcting codes in its dualized form [5,6]. The Floquet version of the quantum Ising model has been central to studies of topology in driven systems [7–10], time crystals [11,12], many-body localization [11,13], and, in its fermionized form, Majorana π modes [14]. A recent experiment on a superconducting quantum processor [15] reveals that temporal spin correlations of the one-dimensional Floquet quantum Ising model can be remarkably robust against certain types of disorder.

In one dimension and in the absence of disorder, the Floquet quantum Ising model is defined through the Floquet operator

$$U_{F,0} = e^{\frac{i\pi g}{2}\sum_{j=1}^{N} X_j} e^{\frac{i\pi J}{2}\sum_{j=1}^{N-1} Z_j Z_{j+1}}, \tag{1}$$

which describes the stroboscopic time evolution of an initial state $|\psi(0)\rangle$ of N qubits through $|\psi(t)\rangle = (U_{F,0})^t|\psi(0)\rangle$ with $t \in \mathbb{N}$. The Floquet operator $U_{F,0}$ can be implemented on a superconducting quantum processor through a set of single- and two-qubit gates. The two-qubit gates effect the Ising exchange coupling involving the Pauli-Z operators of the qubits, while the single-qubit gates realize the transverse field in terms of the Pauli-X operators. The model exhibits four topologically distinct phases as a function of the transverse field g and the exchange coupling J [16–19]. This can be seen by diagonalizing $U_{F,0}$ by a Jordan-Wigner mapping to the Floquet Kitaev chain, a free-fermion model.

For periodic boundary conditions, the single-particle eigenstates of the associated Bogoliubov-de Gennes Floquet operator can be labeled by momentum. The corresponding spectrum of eigenphases $\epsilon \in [-\pi, \pi]$ is shown in Fig. 1(a). One finds two gaps, one around $\epsilon = 0$ and another around $\epsilon = \pm\pi$, which can both be trivial or topological. This results in the four possible phases displayed in the phase diagram in Fig. 1(b) [16,17].

In an open chain, the two types of topological gaps are signaled by a pair of Majorana zero modes (MZMs) or Majorana π modes (MPMs), respectively [14]. These modes appear in the middle of the corresponding gap and exhibit a hybridization splitting away from $\epsilon = 0$ (MZMs) or $\epsilon = \pm\pi$ (MPMs) by an amount which is exponentially small in the length N of the chain, see Fig. 1(c). In the presence of the Majorana modes, the corresponding many-body Floquet eigenstates of $U_{F,0}$ have eigenphases that come in pairs. Apart from hybridization splittings, the paired eigenphases are degenerate (MZMs) or shifted relative to each other by π (MPMs), see Fig. 1(d). This is a particular instance of the wider phenomenon of strong modes in interacting and kicked spin models [20–24].

The Floquet quantum Ising model and its fermionized version can be implemented in a variety of platforms including cold atomic gases [14], wide Josephson junctions [25], and quantum wires [16,17,26]. Motivated by the recent implementation on a superconducting quantum information processor [15], we study the effects of quenched random fields on the MZM and MPM-induced pairings of eigenphases as well as the ramifications for temporal spin-spin correlation functions. This is of considerable interest for two reasons. First, inaccuracies in implementing the gate operations naturally introduce a certain degree of randomness, making robustness against
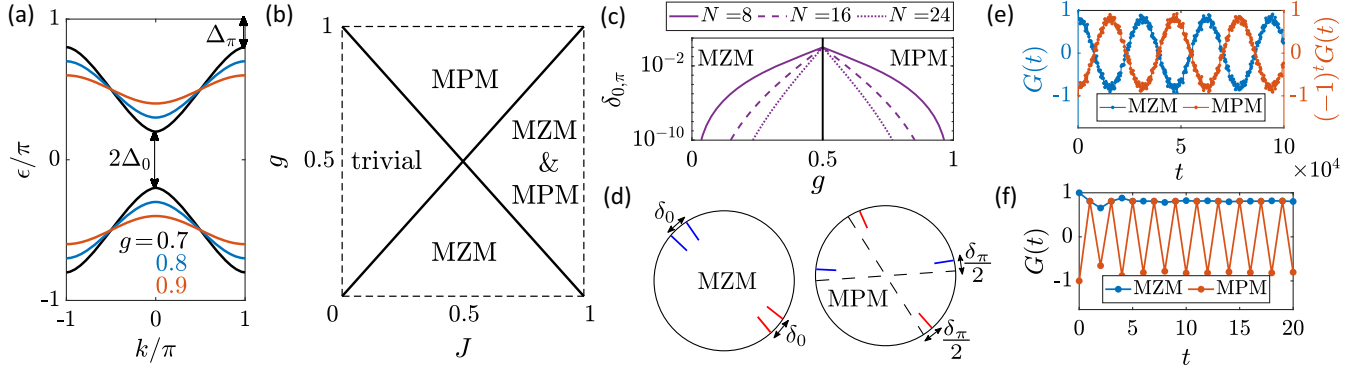
FIG. 1.   Clean quantum Ising chain. (a) Single-particle Floquet spectrum of a periodic chain vs wave vector k for various transverse fields g. (b) Phase diagram with phases labeled by the Majorana modes present in the corresponding Kitaev chain. (c) Hybridization splitting $\delta_{0,\pi}$ vs g of Majorana modes in finite chains of various lengths N ($J = 0.5$), showing the symmetry between MZM and MPM phases. (d) Sketch of the pairing of many-body eigenphases in the MZM and MPM phases. Both pairings coexist in the MZM & MPM phase. (e),(f) Spin-spin correlation function $G(t)$ for (e) long [note the factor $(-1)^t$ for the MPM phase] and (f) short times. For long times, $G(t)$ oscillates with period $2\pi/\delta_{0,\pi}$, superimposed on rapid period-two oscillations in the MPM phase. Parameters: (a) $J = 0.5$, (e),(f) $N = 8$, $(g, J) = (0.2, 0.5)$ (MZM), $(g, J) = (0.8, 0.5)$ (MPM).

disorder an important issue in experiment and applications. Second, in the context of studying strong modes, disorder raises important theoretical questions, especially because a random longitudinal field involving the Pauli-Z operators breaks the protecting spin-flip symmetry of the clean quantum Ising model. Remarkably, we find that longitudinal disorder can even strengthen the spectral π pairing, a result which extends beyond the robustness observed in experiment [15]. We uncover dramatic differences between MZMs and MPMs, which may make the latter particularly interesting in the context of quantum information processing.

Random transverse field.—We begin by studying random transverse fields and consider the Floquet operator $U_F = U_g U_{F,0}$ with $U_g = \exp\{(i\pi/2)\sum_{j=1}^N g_j X_j\}$. The random fields g_j are drawn from independent box distributions, $g_j \in [-dg, dg]$. Unlike in related models of Floquet time crystals [11,12,27–33], we consider a fixed J. Given that U_g describes a field that is random in space but independent of time t, the disordered model remains Floquet and is characterized by a many-body spectrum of 2^N eigenphases E_n on the unit circle, $U_F|n\rangle = e^{-iE_n}|n\rangle$.

In the presence of the random transverse field, one can still find a set of N fermionic Bogoliubov operators γ_α satisfying [15,16,34] (as reviewed in the Supplemental Material [19])

$$U_F^\dagger \gamma_\alpha U_F = e^{-i\epsilon_\alpha}\gamma_\alpha. \tag{2}$$

This can, e.g., be done by expressing the spins in Jordan-Wigner fermions and a subsequent Bogoliubov transformation. Then, the 2^N many-body eigenphases $E_n = \sum_\alpha n_\alpha \epsilon_\alpha$ of U_F can be decomposed into the N single-particle

eigenphases ϵ_α. Here, the $n_\alpha \in \{0, 1\}$ denote occupations $\gamma_\alpha^\dagger \gamma_\alpha$ of the Bogoliubov fermions. Both E_n and ϵ_α are defined modulo 2π. The above-mentioned zero (π) pairing of many-body states follows from the existence of a pair of MZMs (MPMs), which combine into a Bogoliubov fermion γ_0 (γ_π). The corresponding eigenphase ϵ_0 (ϵ_π) differs from zero (π) by an amount δ_0 (δ_π) that is exponentially small in the length of the chain. This leads to deviations from the perfect zero (π) pairing of many-body states by δ_0 (δ_π), which are identical for all pairs of the many-body spectrum.

Random transverse fields induce a broad distribution of the splittings δ_0 and δ_π across the disorder ensemble, which we find to be log-normal. Just as for the splittings in the clean model [see Fig. 1(c)], we find that the log-normal distribution for δ_0 at g is identical to the distribution of δ_π at $g \to 1 - g$. This is illustrated in Figs. 2(a) and 2(b), which show the average and variance of $\ln \delta_{0,\pi}$ as a function of N for corresponding locations in the MZM and MPM phases. The linear dependence on N reflects the exponential dependence of the hybridization splitting. The Supplemental Material [19] gives analytical expressions drawing on the related Hamiltonian problem [35].

Random longitudinal field.—We now turn to the case of a random longitudinal field as described by the Floquet operator $U_F = U_h U_{F,0}$, where $U_h = \exp\{(i\pi/2)\sum_{j=1}^N h_j Z_j\}$ and the random fields h_j are drawn from independent box distributions, $h_j \in [-dh, dh]$. Longitudinal fields differ fundamentally from transverse fields in two ways. First, longitudinal fields do not conserve the spin-flip symmetry $P = \prod_j X_j$ of $U_{F,0}$, which maps to conservation of fermion parity $P = \prod_\alpha (1 - 2\gamma_\alpha^\dagger \gamma_\alpha)$ in the Floquet Kitaev chain. As a result, longitudinal fields directly couple the two many-body states within a pair. Second, the fermionic representations of
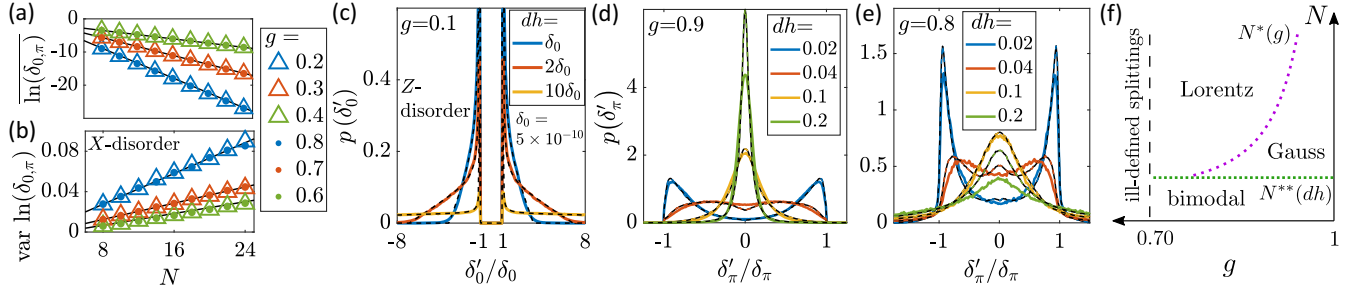
FIG. 2. (a),(b) Random transverse fields: (a) Average and (b) variance of $\ln \delta_{0,\pi}$ vs chain length N for both MZMs ($g < 1/2$; triangles) and MPMs ($g > 1/2$; dots). Numerical results (symbols) are in excellent agreement with analytical expressions (full lines) [19]. (c)–(e) Random longitudinal fields: Splitting distributions for various disorder strengths in (c) MZM and (d),(e) MPM phase. In (c), numerical results (full lines) are well reproduced by an analytical two-level approximation (dashed lines). In (d),(e), numerical results (full lines) can be interpreted in terms of second-order Floquet perturbation theory (dashed lines). (f) "Phase diagram" of the splitting distribution (MPM phase) in the N–g plane for fixed dh. Parameters: $J = 0.5$, (a),(b) $dg = 0.02$, $\mathcal{N} = 10^4$ realizations, (c) $\delta_0 = 5 \times 10^{-10}$, (d) $\delta_\pi = 5 \times 10^{-10}$, (e) $\delta_\pi = 2 \times 10^{-6}$, (c)–(e) $N = 12$, $\mathcal{N} = 10^3$.

the Pauli-Z operators involve string operators, turning the Floquet quantum Ising model with longitudinal disorder into an interacting fermion problem.

Our numerics show that in stark contrast to transverse fields, random longitudinal fields affect the zero and π splittings in dramatically different ways. In the MZM phase, even tiny random longitudinal fields of the order of δ_0 enhance the splittings as shown in Fig. 2(c). We also find that the splittings remain approximately uniform across the many-body spectrum. In contrast, in the MPM phase, random longitudinal fields of order δ_π have essentially no effect. Even fields approaching order unity barely enlarge the splittings δ_π. The splittings are strictly reduced when g is sufficiently close to unity [Fig. 2(d)] and remain concentrated around zero when g is further from unity [Fig. 2(e)]. The splittings vary across the many-body spectrum and are self-averaging [19].

The remarkable robustness of MPMs against a random longitudinal field (as well as the sensitivity of MZMs) can be understood within a low-order stroboscopic Floquet perturbation theory for $U_F = e^{-iV} U_{F,0}$. Expanding the eigenphases of U_F to quadratic order in V, we find $E_n = E_{n,0} + E_{n,1} + E_{n,2} + \cdots$, with [19]

$$E_{n,1} = \langle n_0|V|n_0\rangle; \qquad E_{n,2} = \sum_{m \neq n} \frac{|\langle n_0|V|m_0\rangle|^2}{2 \tan \frac{E_{n,0}-E_{m,0}}{2}}. \quad (3)$$

Here, we assume nondegenerate eigenstates $|n_0\rangle$ of $U_{F,0}$ with eigenphases $E_{n,0}$. For degenerate eigenstates, one first diagonalizes V within the degenerate subspace. Importantly, coupling to a close-by level with small eigenphase difference δ_0 gives a small denominator in $E_{n,2}$. In contrast, coupling to a level with eigenphase difference $\pi - \delta_\pi$ close to π gives a large eigenphase denominator $\tan[(\pi - \delta_\pi)/2] \simeq (2/\delta_\pi)$. Indeed, the two states repel both ways around the unit circle [see Fig. 1(d)], suppressing the second-order correction and pushing the splitting closer to

π. As we show below, π pairings remain much more robust than zero pairings for many-level systems.

As the Z_j are odd under the spin-flip (fermion-parity) symmetry P, a longitudinal field $V = (\pi/2) \sum_{j=1}^N h_j Z_j$ generically has a nonzero matrix element $\langle n_0^e|V|n_0^o\rangle$ coupling partner states, but zero diagonal matrix elements. Here, we denote the two paired many-body eigenstates of $U_{F,0}$ as $|n_0^e\rangle$ and $|n_0^o\rangle$. They have the same occupations $\gamma_\alpha^\dagger \gamma_\alpha$ except for the Majorana occupation $n_{0,\pi} = \gamma_{0,\pi}^\dagger \gamma_{0,\pi}$, with $n_{0,\pi} = 0$ for $|n_0^e\rangle$ and $n_{0,\pi} = 1$ for $|n_0^o\rangle$.

In the MZM phase, we can restrict to the two paired levels provided that hybridization splitting and perturbation are small compared to the level spacing of the many-body spectrum. Diagonalizing the Hamiltonian within this near-degenerate subspace gives the perturbed splitting $\delta_0' = \sqrt{\delta_0^2 + 4|\langle n_0^e|V|n_0^o\rangle|^2}$. This interpolates between second- and first-order perturbation theory as the random field V increases. The eigenstates evolve into perturbed eigenstates $|n_\pm\rangle \simeq (1/\sqrt{2})(|n_0^e\rangle \pm |n_0^o\rangle)$, once the perturbation exceeds δ_0. With this understanding, we derive an analytical splitting distribution [19], which is in excellent agreement with numerical results [Fig. 2(c)]. Here, the square-root singularity of the splitting distribution at $\delta_0' = \delta_0$ is generic, while the bulk of the distribution is sensitive to the choice for the distribution of the random fields.

In the MPM phase, the coupling between the two π-paired states is negligible. Thus, we retain coupling between states belonging to different pairs. Evaluating the splittings $\delta_n = E_n^e - E_n^o + \pi$ in second-order perturbation theory, we find

$$\delta_n \simeq \delta_\pi + \sum_m \left\{ \frac{|\langle n_0^e|V|m_0^o\rangle|^2}{2 \tan \frac{E_n^e - E_m^o}{2}} - \frac{|\langle n_0^o|V|m_0^e\rangle|^2}{2 \tan \frac{E_n^o - E_m^e}{2}} \right\}$$
$$+ \sum_{m \neq n} \left\{ \frac{|\langle n_0^e|V|m_0^e\rangle|^2}{2 \tan \frac{E_n^e - E_m^e}{2}} - \frac{|\langle n_0^o|V|m_0^o\rangle|^2}{2 \tan \frac{E_n^o - E_m^o}{2}} \right\}. \quad (4)$$
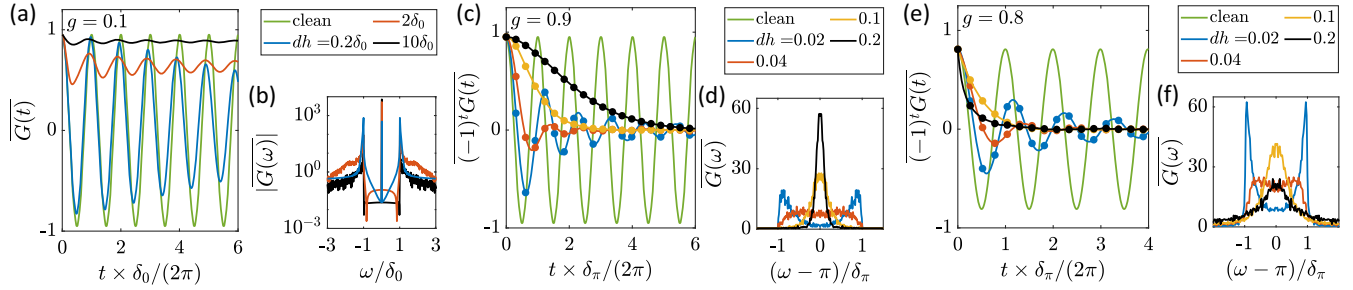
FIG. 3. Boundary spin-spin correlation function $G(t)$ and its Fourier transform $G(\omega)$ with random longitudinal fields (see legends for strength). (a),(b) MZM phase: The random field suppresses the oscillations induced by the finite splitting δ_0 and generates a constant ($\omega = 0$) contribution. (c) MPM phase at $g = 0.9$: The random field suppresses the oscillations induced by δ_π in $(-1)^t G(t)$. The decay is Gaussian for large disorder and becomes slower with increasing dh. The correlation function (markers) is well reproduced when restricting the summation in Eq. (6) to π-paired states n and m, and (d) $G(\omega)$ approximately tracks the δ'_π distribution, cf. Fig. 2(d). (e),(f) MPM phase at $g = 0.8$: $(-1)^t G(t)$ now decays exponentially reflecting the Lorentzian δ'_π distribution. Parameters: $J = 0.5$, $N = 12$, $\mathcal{N} = 10$, (a)–(d) $\delta_0 = \delta_\pi = 5 \times 10^{-10}$, (e),(f) $\delta_\pi = 2 \times 10^{-6}$.

We have made second-order perturbation theory self-consistent by inserting the exact eigenphases $E_n^{e,o}$ in the denominators. This is motivated by the observation that there are couplings between many different pairs, which are of similar magnitude and can thus plausibly be accounted for in a self-consistent scheme. Linearizing Eq. (4) in the small splittings δ_n, it can be readily solved numerically [19]. Figure 2(d) shows that the resulting splitting distribution reproduces exact diagonalization data remarkably well over a wide range of disorder strengths. In particular, one reproduces the crossover from a bimodal distribution peaked near the splittings of the clean system to a narrower distribution peaked at $\delta'_\pi = 0$ [Figs. 2(d) and 2(e)] with increasing disorder dh. We observe that the distribution peaked at $\delta'_\pi = 0$ is approximately Gaussian, when g is sufficiently close to unity, but becomes Lorentzian for larger $1 - g$.

A corresponding "phase diagram" is shown in Fig. 2(f), which can be understood from Eq. (4). For g close to unity, the second sum on the right-hand side can be dropped. Then, expanding in the δ_n, we find $\delta_n = \delta_\pi - \sum_m (\delta_n + \delta_m)\Sigma_{nm}$, where the

$$\Sigma_{nm} = \frac{|\langle n_0^e|V|m_0^o\rangle|^2}{4\cos^2 \frac{E_n^e - E_m^e}{2}} \quad (5)$$

are strictly positive. Setting $\delta_n \approx \delta_{\mathrm{typ}}$ as well as $\delta_m \approx \pm\delta_{\mathrm{typ}}$, the typical splitting $\delta_{\mathrm{typ}} \approx \delta_\pi/(1 + \langle\sum_m \Sigma_{nm}\rangle_n)$ is indeed reduced compared to δ_π. ($\langle\ldots\rangle_n$ is an average over n.) The crossover between the bi- and unimodal distributions occurs when $\Sigma \sim 1$, implying $N^{**} \propto \ln(1/dh)$, approximately independent of g [19].

As g deviates further from unity, the single-particle band broadens [Fig. 1(a)]. Consequently, the many-body eigenphases cover the entire interval $[-\pi, \pi]$ when $N > N^* \sim 1/(1 - g)^2$. In this regime, the second term on the right-hand side of Eq. (4) becomes significant

due to the appearance of small denominators. The Lorentzian distribution can then be interpreted as an instance of a stable Levy distribution [19,36]. We note that the splitting is well defined when the Majorana splitting $\sim e^{-N/\xi}$ is small compared to the many-body level spacing $\sim 2^{-N}$, where ξ is the correlation length of the clean model, a condition satisfied for $g > 0.71$ at $J = 0.5$.

Boundary spin-spin correlations.—We finally consider the boundary spin-spin correlation function

$$G(t) = \frac{1}{2^N}\mathrm{tr}\{Z_1(t)Z_1(0)\} = \frac{1}{2^N}\sum_{n,m}|(Z_1)_{nm}|^2 e^{-iE_{nm}t}, \quad (6)$$

averaged over all initial states. Here, $(Z_1)_{nm} = \langle n|Z_1|m\rangle$ and $E_{nm} = E_n - E_m$. Sums are over all 2^N many-body eigenstates. In the MZM phase of the clean model, the pairing of eigenphases makes $G(t)$ oscillate with an exponentially long period $1/\delta_0$, [Fig. 1(e)]. In the MPM phase, the slow oscillations with period $1/\delta_\pi$ modulate rapid period-two oscillations [Fig. 1(f)].

Experimentally, $G(t)$ in the presence of a random longitudinal field persists up to times of the order of the qubit lifetime ($\ll 1/\delta_{0,\pi}$) regardless of the phase [15]. This is surprising given the dramatically different sensitivities of the zero and π pairings to longitudinal disorder. In fact, we find that the reasons underlying the robustness of $G(t)$ are very different in the two phases and that the long-time behaviors are actually quite distinct.

In the MZM phase, the longitudinal field effectively polarizes the boundary spins. Spins located away from the boundary remain unpolarized due to the presence of mobile domain walls in generic states. Correspondingly, first-order degenerate perturbation theory gives perturbed eigenstates $|n_\pm\rangle$, which have nonzero diagonal matrix elements of Z_1 and Z_N. Then, the boundary spin-spin correlation function in Eq. (6) has diagonal and thus time-independent terms,

once the perturbation is large compared to the exponentially small splitting [Fig. 3(a)]. The Fourier transform of the boundary spin-spin correlation function develops a dominant zero-frequency peak [Fig. 3(b)]. In parallel, longitudinal disorder rapidly suppresses the amplitude of the Majorana oscillations.

In the MPM phase, we observe that the period-two oscillations persist in the presence of a random longitudinal field, while the slow oscillation of their envelope decays, see Figs. 3(c) and 3(e). This can be understood as a consequence of the splitting distribution across the many-body spectrum akin to inhomogeneous broadening. In fact, $G(t)$ in Eq. (6) is dominated by terms, in which $|n\rangle$ and $|m\rangle$ are π-paired states [Figs. 3(c) and 3(e)]. Then, the envelope of $G(t)$ is effectively the Fourier transform of the splitting distribution [Figs. 3(d) and 3(f)]. Damped oscillations of the envelope persist for a bimodal distribution, with a long-time power-law tail due to the hard cutoff of the splitting distribution at $\delta'_\pi = \delta_\pi$. This gives way to a nonoscillatory Gaussian (exponential) decay in the Gaussian (Lorentzian) regimes of the splitting distribution [Fig. 2(f)]. Thus, in the MPM phase, $G(t)$ directly reflects the robustness of the π pairing to a random longitudinal field.

Conclusions.—We showed that even in the presence of random longitudinal fields far exceeding the nominal MPM splitting δ_π, the π pairing of the MPM phase remains exponentially precise in the system size N. We explain this surprising robustness, which contrasts sharply with the sensitivity of the zero pairing in the MZM phase, in terms of level repulsion of many-body Floquet levels on the unit circle, without invoking the notion of prethermalization [15,21,37]. Our work also points towards the importance of unconventional level statistics such as the distribution of π splittings in Floquet systems.

It has been suggested to exploit the zero pairing in the quantum Ising model for realizing qubits, e.g., by implementing the model in chains of Josephson junctions [38–40]. However, unlike the closely related Majorana qubits [41–43], there would be no protection against symmetry-breaking longitudinal fields. This may make the remarkable robustness of π pairing interesting for applications in quantum information processing.

[1] P. Pfeuty, Ann. Phys. (Leipzig) **57**, 79 (1970).

[2] S. Sachdev, *Quantum Phase Transitions*, 2nd ed. (Cambridge University Press, Cambridge, 2011).

[3] D. S. Fisher, Phys. Rev. B **51**, 6411 (1995).

[4] A. Y. Kitaev, Phys. Usp. **44**, 131 (2001).

[5] J. B. Kogut, Rev. Mod. Phys. **51**, 659 (1979).

[6] A. Y. Kitaev, in *Proceedings of the 3rd International Conference of Quantum Communication and Measurement*, edited by O. Hirota, A. S. Holevo, and C. M. Caves (Plenum, New York, 1997).

[7] C. W. von Keyserlingk and S. L. Sondhi, Phys. Rev. B **93**, 245145 (2016).

[8] C. W. von Keyserlingk and S. L. Sondhi, Phys. Rev. B **93**, 245146 (2016).

[9] A. Russomanno, B.-E. Friedman, and E. G. Dalla Torre, Phys. Rev. B **96**, 045422 (2017).

[10] A. Mitra, H.-C. Yeh, F. Yan, and A. Rosch, Phys. Rev. B **107**, 245416 (2023).

[11] V. Khemani, A. Lazarides, R. Moessner, and S. L. Sondhi, Phys. Rev. Lett. **116**, 250401 (2016).

[12] D. V. Else, B. Bauer, and C. Nayak, Phys. Rev. Lett. **117**, 090402 (2016).

[13] W. Berdanier, M. Kolodrubetz, S. A. Parameswaran, and R. Vasseur, Proc. Natl. Acad. Sci. U.S.A. **115**, 9491 (2018).

[14] L. Jiang, T. Kitagawa, J. Alicea, A. R. Akhmerov, D. Pekker, G. Refael, J. I. Cirac, E. Demler, M. D. Lukin, and P. Zoller, Phys. Rev. Lett. **106**, 220402 (2011).

[15] X. Mi *et al.*, Science **378**, 785 (2022).

[16] M. Thakurathi, A. A. Patel, D. Sen, and A. Dutta, Phys. Rev. B **88**, 155133 (2013).

[17] B. Bauer, T. Pereg-Barnea, T. Karzig, M.-T. Rieder, G. Refael, E. Berg, and Y. Oreg, Phys. Rev. B **100**, 041102(R) (2019).

[18] A. Lerose, M. Sonner, and D. A. Abanin, Phys. Rev. B **104**, 035137 (2021).

[19] See Supplemental Material at http://link.aps.org/supplemental/10.1103/PhysRevLett.132.210401 for details on the exact solution of the quantum Ising model, random transverse fields, stroboscopic Floquet perturbation theory, and self-consistent perturbation theory for the MPM phase.

[20] P. Fendley, J. Phys. A **49**, 30LT01 (2016).

[21] D. V. Else, P. Fendley, J. Kemp, and C. Nayak, Phys. Rev. X **7**, 041062 (2017).

[22] J. Kemp, N. Y. Yao, C. R. Laumann, and P. Fendley, J. Stat. Mech. (2017) 063105.

[23] D. J. Yates, F. H. L. Essler, and A. Mitra, Phys. Rev. B **99**, 205419 (2019).

[24] H.-C. Yeh, A. Rosch, and A. Mitra, Phys. Rev. B **108**, 075112 (2023).

[25] D. T. Liu, J. Shabani, and A. Mitra, Phys. Rev. B **99**, 094303 (2019).

[26] A. Matthies, J. Park, E. Berg, and A. Rosch, Phys. Rev. Lett. **128**, 127702 (2022).

[27] C. W. von Keyserlingk, V. Khemani, and S. L. Sondhi, Phys. Rev. B **94**, 085112 (2016).

[28] N. Y. Yao, A. C. Potter, I.-D. Potirniche, and A. Vishwanath, Phys. Rev. Lett. **118**, 030401 (2017).

[29] X. Mi *et al.*, Nature (London) **601**, 531 (2021).

[30] K. Sacha and J. Zakrzewski, Rep. Prog. Phys. **81**, 016401 (2017).

[31] V. Khemani, R. Moessner, and S. L. Sondhi, arXiv:1910.10745.

[32] D. V. Else, C. Monroe, C. Nayak, and N. Y. Yao, Annu. Rev. Condens. Matter Phys. **11,** 467 (2020).

[33] M. P. Zaletel, M. Lukin, C. Monroe, C. Nayak, F. Wilczek, and N. Y. Yao, Rev. Mod. Phys. **95,** 031001 (2023).

[34] H. Ling, P. Richard, S. R. Koshkaki, M. Kolodrubetz, D. Meidan, A. Mitra, and T. Pereg-Barnea, Phys. Rev. B **109,** 155144 (2024).

[35] P. W. Brouwer, M. Duckheim, A. Romito, and F. von Oppen, Phys. Rev. Lett. **107,** 196804 (2011).

[36] J.-P. Bouchaud and A. Georges, Phys. Rep. **195,** 127 (1990).

[37] D. A. Abanin, W. De Roeck, W. W. Ho, and F. Huveneers, Phys. Rev. B **95,** 014112 (2017).

[38] C. Bruder, R. Fazio, and G. Schön, Phys. Rev. B **47,** 342 (1993).

[39] L. S. Levitov, T. P. Orlando, J. B. Majer, and J. E. Mooij, arXiv:cond-mat/0108266.

[40] J. Q. You, Z. D. Wang, W. Zhang, and F. Nori, Sci. Rep. **4,** 5535 (2014).

[41] S. Plugge, A. Rasmussen, R. Egger, and K. Flensberg, New J. Phys. **19,** 012001 (2017).

[42] T. Karzig, C. Knapp, R. M. Lutchyn, P. Bonderson, M. B. Hastings, C. Nayak, J. Alicea, K. Flensberg, S. Plugge, Y. Oreg, C. M. Marcus, and M. H. Freedman, Phys. Rev. B **95,** 235305 (2017).

[43] Y. Oreg and F. von Oppen, Annu. Rev. Condens. Matter Phys. **11,** 397 (2020).

[44] L. Bennett, B. Melchers, and B. Proppe, Curta: A general-purpose high-performance computer at ZEDAT, Freie Universität Berlin, 2020.